Received: December 18, 2021. Revised: February 23, 2022.

INASS

International Journal of
Intelligent Engineering & Systems

http://www.inass.org/

Fractional Order Fuzzy PID Controller Design for 2-Link Rigid Robot Manipulator

Hadeel I. Abdulameer[1]* **Mohamed J. Mohamed[1]**

[1]*Control and Systems Engineering Department, University of Technology, Baghdad, Iraq*
* Corresponding author's Email: cse.19.13@grad.uotechnology.edu.iq

Abstract: In this paper, we present four control structures for the Fractional/Integer Order Fuzzy Proportional Integral Derivative controllers that are used for a 2-link rigid robot manipulator. The manipulator is dealing with the trajectory tracking problem. A metaheuristic optimization technique, namely the most valuable player algorithm, is presented to optimize the controller's parameters while minimizing the integral of time square error. Furthermore, the proposed controllers' robustness is examined for changing the initial condition, exterior disturbances, and parameter variations. MATLAB code outcomes show that the Fractional Order Fuzzy Proportional Integral Derivative controllers ensure the best trajectory tracking and also improve the system's robustness to change the initial condition, external disturbances, and parameter variations. The best structure is the Fractional Order Fuzzy Proportional Derivative -Fractional Order Proportional Integral Derivative controller among all structures with the minimum integral of time square error that is equal to 7.7481×10-5 for trajectory tracking, 2.4334×10-5 for changing of the initial position, 2.1893×10-4 for disturbances rejection and 2.4990×10-6 for parameter variation. The result showed also that the response of the trajectory tracking for theta1 and theta2 without overshoot and it has minimum settling time in the case of Fractional Order Fuzzy Proportional Derivative -Fractional Order Proportional Integral Derivative controller.

Keywords: Fractional-order controller, Fuzzy logic, Most valuable player algorithm, PID controller, Robotic manipulator.

1. Introduction

Robotics is the branch of science concerned with the design, simulation, and control of robots. Nowadays robots are being used in almost every aspect of daily life. It has accompanied people in most of the industry and daily life jobs [1]. A very wide range of applications was found, which include cargo loading and unloading, automatic assembly lines, spray paint application, handling dangerous radioactive materials, forging, and military use. It is well known that robot arm dynamics are highly nonlinear and require expensive computations [2].

During its operations, the robotic manipulator is subjected to external disturbances, a variety of uncertainties, parameter variations, and payload modifications in addition to the complexity and nonlinearity difficulties. As a result, traditional proportional-integral-derivative (PID) controllers are not capable of providing simultaneous effective control for trajectory tracking and constant force/twist control [3].

Various controllers have been suggested for a 2-link rigid robot manipulator (2-LRRM) by several authors. A fuzzy controller and different conventional control techniques like PD, PID, and computed torque control were proposed in [4]. When compared to conventional controllers, the fuzzy controller provided the best performance and the most effective and accurate trajectory tracking capability. The main issues of this study were that the robust concept does not achieve and the parameters of the controller were not optimized by any optimization method. In [5] a Fractional Order Fuzzy Proportional-Integral-Derivative (FOFPID) controller for a two-link planar rigid robotic manipulator was presented for the trajectory

tracking problem. The robustness of the FOFPID controller was tested for model uncertainties, disturbance rejection, and noise suppression. Its performance was compared with the other three controllers namely Fuzzy PID (FPID), Fractional Order PID (FOPID), and conventional PID. Numerical simulation results showed that the FOFPID controller outperforms competing controllers.

The PD neural network (NN)-based adaptive controller design for robotic manipulators trajectory tracking, is subject to noise measurement and external disturbances, which was presented in [6], the results showed that the neural network modification of the adaptation laws of the weights gave batter performance in function approximation and thus better performance of the controller compared to the ideal adaptation law. The modification includes e-modification and σ-modification. The issue was that the parameters of the controller were not optimized by any optimization method.

A Fractional-Order Fuzzy Proportional Integral-Fractional Order Derivative Filter (FOFPI-D) for controlling a nonlinear two-link robotic manipulator system was introduced in [7]. Fuzzy proportional integral-derivative filter (FPI-D) and proportional integral-derivative filter (PI-D) controllers were also prepared to compare their results with that of the FOFPI-D. The results were shown that the FOFPI-D controller outperforms other designed controllers. In [8] an adaptive neural network (NN) for feed-forward compensation is used alongside a sectorial fuzzy controller SFC in the feedback loop to control the trajectory tracking of the robot manipulator. The results were presented in comparison with the PD plus feed-forward controller, feed-forward SFC, and feed-forward adaptive neural nonlinear PD control. The suggested controller outperforms its competitors, the main problems were that the robust concept does not achieve and the controller didn't eliminate the chattering property in the control signal. The fuzzy-neural-network PID (FNN- PID) control framework of the robotic manipulator was introduced in [3]. A fuzzy neural network algorithm was proposed to adjust the PID controller parameters effectively and quickly. Computer simulations were conducted and examined to demonstrate the proposed method's efficiency. In [9] three types of dynamic control strategies are used for the PUMA 560 robot manipulator. The strategies are PID, Sliding Mode Control (SMC), and Integral Sliding Mode Control (ISMC). The strategies were proposed based on Particle Swarm Optimization (PSO) Algorithm. Simulation results showed that the proposed tuning method achieved a high level of stability, as well as an excellent implementation of the proposed strategy for the PUMA robot. A robust type-2 adaptive control had been developed for the trajectory tracking of an industrial 3-DOF manipulator robot in faulty conditions in [10]. The adaptation involves using Lyapunov stability concepts to update fuzzy type-2 parameters online. The simulation results of the proposed control strategy showed that it was capable of delivering a small tracking error even when payload variation and actuator defects were present.

This work will use four structures of the Fractional/Integer Order Fuzzy PID controller (FOFPID, IOFPID), combining the fractional-order actions will increase the robustness of the controller, hence a more powerful and flexible design method could be developed to meet the specifications of the controlled system [11]. The most valuable player algorithm (MVPA) is adopted to find the best values of the controller's parameters. A comparison between the performance of FOFPID controllers and IOFPID controllers has been made and the obtained results have been presented.

The main contributions of the proposed controllers are highlighted as follows:

1- Four structures of the Fractional/Integer Order Fuzzy PID controllers are designed at the same work.
2- Compared with [4, 6] who did not use the optimal values of the controller, instead, MVPA is used to get the optimum values for the controllers.
3- The robustness of the proposed controllers is demonstrated by changing the initial condition, external disturbances, and parameter variations which are not demonstrated in [4, 8].
4- The control signals of the proposed controllers have no chattering while in [8] there is chattering in the control signal.
5- In comparison with [5, 7], the results of the proposed FOFPID controllers are better or converge to the best values obtained from the existing controllers.

The remainder of this work is arranged as follows. In Section 2, the dynamical model of the 2-LRRM is explained. In Section 3, the suggested FOFPID, IOFPID controllers are illustrated. In Section 4 the proposed MVPA is described in detailed steps. The results of the simulation and the conclusion are given in Sections 5 and 6 respectively.

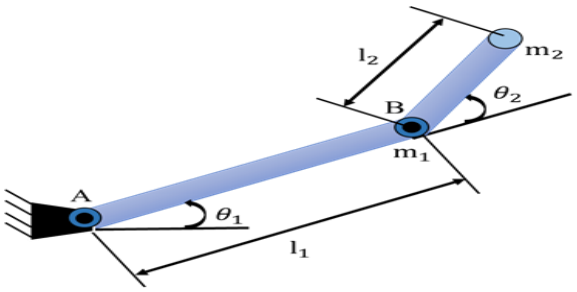

Figure. 1 The structure of 2-LRRM

2. The dynamic model of 2-LRRM

The 2-LRRM scheme is shown in Fig. 1. It consists of two links of lengths l_1 and l_2. Their centers of masses are m_1 and m_2 respectively, that are located at the distal ends of links. To generate the controlling torque at points A and B, DC motors are used to estimate the angular positions ($\theta_1$andθ_2) and velocities ($\dot{\theta}_1$and $\dot{\theta}_2$) of the links, encoders are employed [7].

The manipulator's dynamic equation of motion is used in robotics to set up the basic control equations. The torques generated by the actuators are used to produce the manipulator's arm dynamic motion in a robotic system. The association between the input torques and the time rates of change of the robot arm components configurations characterizes the robotic system dynamic modeling which is concerned with the derivation of the equations of motion of the manipulator as a function of the forces and moments acting on it. As a result, dynamic modeling of a robot manipulator includes specifying the functions that map the forces acting on the structures and the joint positions, velocities, and accelerations [12].

The equations for x- position and y-position of m_1 are given by:

$$x_1 = l_1 \cos(\theta_1) \quad (1)$$

$$y_1 = l_1 \sin(\theta_1) \quad (2)$$

Similarly, the equations for x- position and the y-position of m_2 are given by:

$$x_2 = l_1 \cos(\theta_1) + l_2 \cos(\theta_1 + \theta_2) \quad (3)$$

$$y_2 = l_1 \sin(\theta_1) + l_2 \sin(\theta_1 + \theta_2) \quad (4)$$

The kinetic energy is defined as:

$$KE = \frac{1}{2} m_1(\dot{x}_1^2 + \dot{y}_1^2) + \frac{1}{2} m_2(\dot{x}_2^2 + \dot{y}_2^2) \quad (5)$$

And the potential energy can be written as:

$$PE = m_1 g l_1 \sin(\theta_1) + m_2 g(l_1 \sin(\theta_1) + l_2 \sin(\theta_1 + \theta_2)) \quad (6)$$

Next, by Lagrange Dynamic, we form the Lagrangian which is defined as:

$$L = KE - PE \quad (7)$$

The Euler Lagrange Equation is given by:

$$\frac{d}{dt}\left[\frac{\partial L}{\partial \dot{\theta}_i}\right] - \frac{\partial L}{\partial \theta_i} = F\theta_i \quad (8)$$

Where $F\theta_i$ is the torque applied to the i'th link Lastly, following Lagrange's equation, the dynamics of the arm are given by the two coupled nonlinear differential equations [13]:

$$\begin{aligned}\tau_1 = {} & \left[(m_1 + m_2)l_1^2 + m_2 l_2^2 + 2m_2 l_1 l_2 \cos(\theta_2)\right]\ddot{\theta}_1 + \left[m_2 l_2^2 + m_2 l_1 l_2 \cos(\theta_2)\right]\ddot{\theta}_2 \\ & - m_2 l_1 l_2 \left(2\dot{\theta}_1\dot{\theta}_2 + \dot{\theta}_2^2\right)\sin(\theta_2) + (m_1 + m_2) g l_1 \cos(\theta_1) \\ & + m_2 g l_2 \cos(\theta_1 + \theta_2)\end{aligned} \quad (9)$$

$$\tau_2 = [m_2 l_2^2 + m_2 l_1 l_2 \cos(\theta_2)]\ddot{\theta}_1 + m_2 l_2^2 \ddot{\theta}_2 + m_2 l_1 l_2 \dot{\theta}_1^2 \sin(\theta_2) + m_2 g l_2 \cos(\theta_1 + \theta_2) \quad (10)$$

These manipulator dynamics are in the standard form

$$M(\theta)\ddot{\theta} + V(\theta, \dot{\theta}) + g(\theta) = \tau \quad (11)$$

With $V(\theta, \dot{\theta})$ is the Coriolis/centripetal vector, $M(\theta)$ is the inertia matrix, and $g(\theta)$ is the gravity vector. Note that M (θ) is symmetric.

$$M = \begin{bmatrix} M_{11} & M_{12} \\ M_{21} & M_{22} \end{bmatrix}$$

$$M_{11} = (m_1 + m_2)l_1^2 + m_2 l_2^2 + 2m_2 l_1 l_2 \cos(\theta_2]$$

$$M_{12} = m_2 l_2^2 + m_2 l_1 l_2 \cos(\theta_2]$$

$$M_{12} = M_{21} \quad \& \quad M_{22} = m_2 l_2^2$$

V is the Coriolis and centrifugal matrix which is given by

$$V = \begin{bmatrix} V_1 \\ V_2 \end{bmatrix}$$

$$V_1 = -m_2 l_1 l_2 \left(2\dot{\theta}_1\dot{\theta}_2 + \dot{\theta}_2^2\right)\sin(\theta_2)$$

Table 1. The parameters of 2-LRRM

parameters	Nominal value
m_1	0.1 kg
m_2	0.1 kg
l_1	0.8 m
l_2	0.4 m
g	9.81 m/s^2

$$V_2 = m_2 l_1 l_2 \dot{\theta}_1^2 \sin(\theta_2)$$

The gravity vector $g = [\, g_{12} \quad g_{21} \,]^T$is given by:

$$g_{12} = (m_1 + m_2) g l_1 \cos(\theta_1) + m_2 g l_2 \cos(\theta_1 + \theta_2)$$

$$g_{21} = m_2 g l_2 \cos(\theta_1 + \theta_2)$$

The parameters are considered in Table 1

3. Controller design

Before describing the proposed controllers, we will give a brief overview of the components of these controllers, and then explain the nature and structures of the proposed controllers for the 2-LRRM.

3.1 The components of the proposed controllers

3.1.1. PID controller

The PID controller contains three parts as a style of the feedback control loop, the first part is proportional which is responsible for providing an overall control action that is directly related to the error signal through a gain factor. The second one is the integral part which is used to reduce the steady-state error by using a low-frequency compensation or an integrator. The third and final part is the derivative part which is responsible for improving the transient state response by using a high-frequency compensator or a differentiator [14, 15]. A typical PID controller is called the "three-term" controller. Its transfer function is usually given as Eq. (12).

$$G(s) = K_p + K_i \frac{1}{s} + K_d s \qquad (12)$$

Where K_p is the proportional gain, K_i is the integral gain, K_d is the derivative gain.

3.1.2. Fractional order PID controller

Fractional order PID is one of the most effective controls that are common and useful in practical industries. Podlubny and Oustaloup suggest the fractional order PID controller, namely the PI$^{\lambda}$D$^{\mu}$ or FOPID which is the generalization form of the classical PID controller. They used the fractional order controller to establish the CRONE-controller (Commande Robuste d'Ordre Non-Enterier controller) in their series of papers and books [11]. Non-integer integration and differentiation are described in a variety of ways. The Grünwald–Letnikov (GL) and Riemann–Liouville (RL) definitions, as well as the Caputo definitions, are the most widely used[16].The GL definition is:

$$D_t^{\alpha} f(t) = \lim_{h \to 0} \frac{1}{h^{\alpha}} \sum_{j=0}^{\left[\frac{t-a}{h}\right]} (-1)^j \binom{\alpha}{j} f(t - jh) \qquad (13)$$

While the RL definition is given by:

$${}_aD_t^{\alpha} f(t) = \frac{1}{\Gamma(n-\alpha)} \frac{d^n}{dt^n} \int_a^t \frac{f(\tau)}{(t-\tau)^{\alpha-n+1}} \, d\tau \qquad (14)$$

For $(n-1<\alpha<n)$ and $\Gamma(x)$ is the well-known Euler's Gamma function.

$$g(t, {}_aD_t^{\alpha 1} x, {}_aD_t^{\alpha 2} x, \dots) = 0 \qquad (15)$$

where $\alpha_k \in R^+$.

Caputo's definition can be written as

$${}_aD_t^{\alpha} f(t) = \frac{1}{\Gamma(\alpha-n)} \int_a^t \frac{f^{(n)}}{(t-\tau)^{\alpha-n+1}} \, d\tau \qquad (16)$$

for $(n - 1 < \alpha < n)$

The PI$^{\lambda}$D$^{\mu}$ controller transfer function is given as the ratio of the controller output U(s) and error E(s)[11].

$$G(s) \frac{U(s)}{E(s)} = K_p + K_i s^{-\lambda} + K_d s^{\mu} \quad \lambda, \mu > 0 \qquad (17)$$

By adding more general control behaviors of the PI$^{\lambda}$D$^{\mu}$ type, more acceptable results between the positive and negative effects of traditional PID could be obtained. Furthermore, more flexible and powerful design methods could be developed by collaborating fractional-order actions, to meet the specifications of the controlled system [11].

3.1.3. Fuzzy logic controller (FLC)

To introduce human decision-making and experience to the plant, Fuzzy Logic Controllers (FLCs) are represented to the system to include the intelligence to the controller. A set of linguistic rules or relational expressions are used to represent the relationships between the input and the output [17].

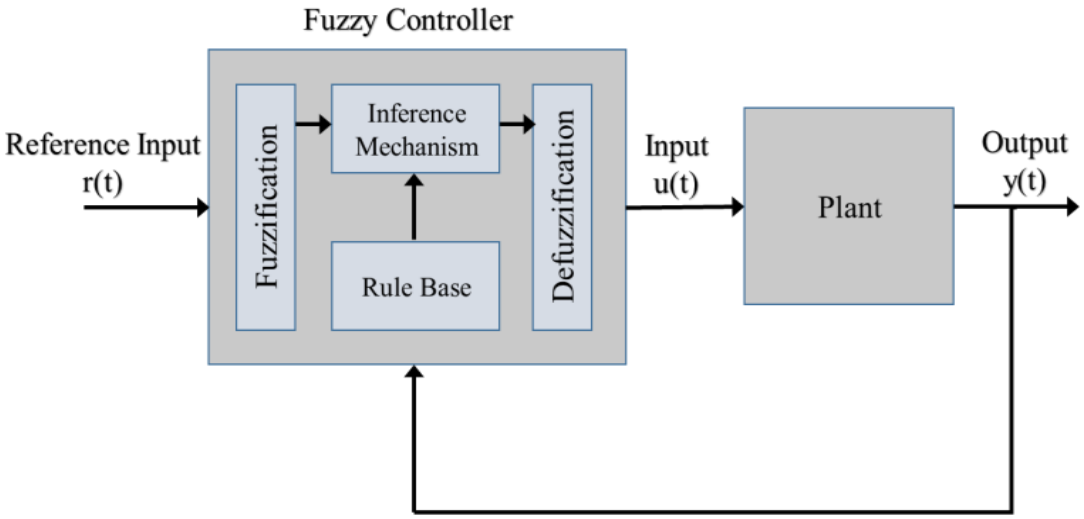

Figure. 2 The structure of the fuzzy controller

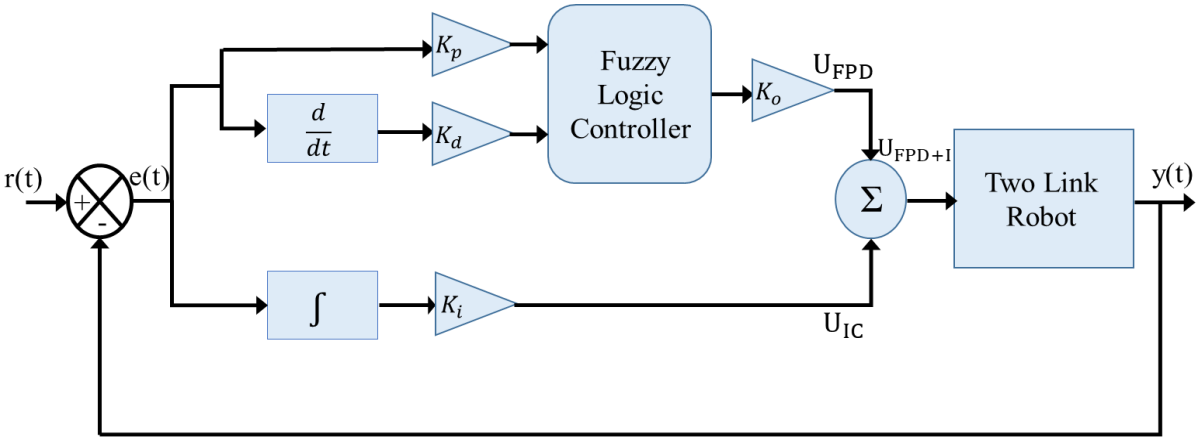

Figure. 3 The Fractional/Integer order fuzzy PD+I controller structure for the 2-LRRM

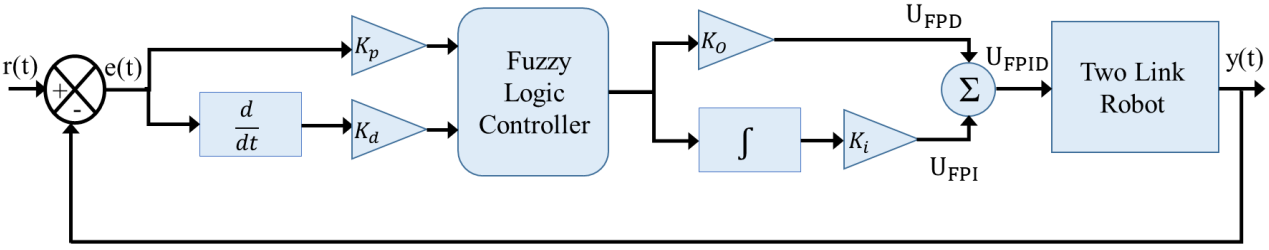

Figure. 4 The structure of the one block Fractional/Integer order fuzzy PID controller for 2-LRRM

A fuzzy logic controller block diagram is given in Fig. 2. The fuzzy controller has four major parts: the first one is the rule-base which contains a set of rules for the most effective control of the system that represents the knowledge. The second part is the inference mechanism which decides which control rules are applicable at the current circumstance and then determines what should be the output of the controller to the plant. The third part is the fuzzification interface which simply modifies the inputs so that they can match the rules of the rule base. The final part is the defuzzification interface that transforms the inference mechanism's conclusions into the inputs to the plant [18, 19].

3.2 The structures of the proposed controller

Four structures of FOFPID and IOFPID controllers are proposed to control the trajectory tracking of the 2-LRRM.

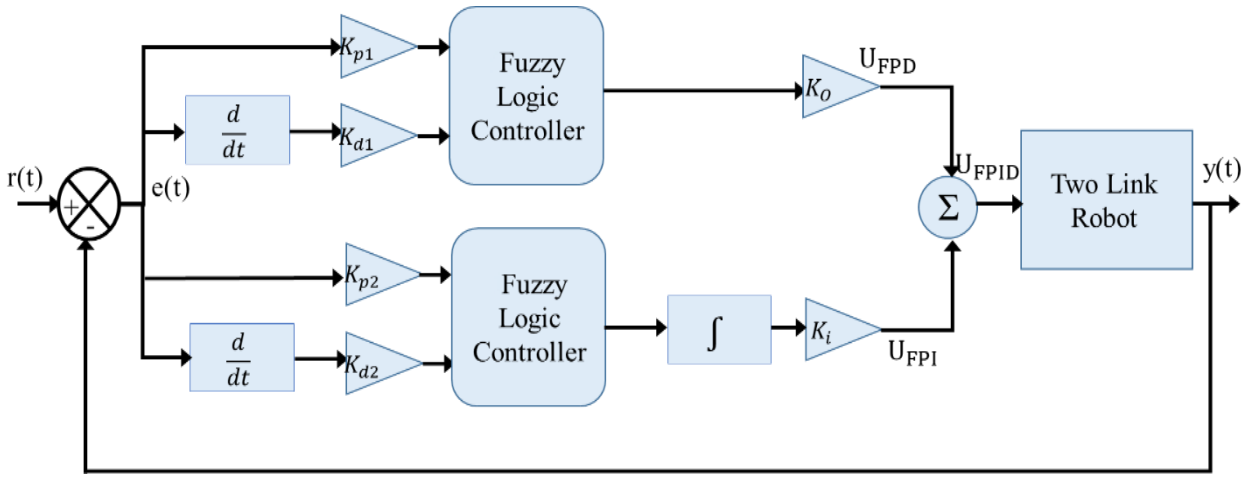

Figure. 5 The structure of the two-block Fractional/Integer order fuzzy PID controller for 2-LRRM

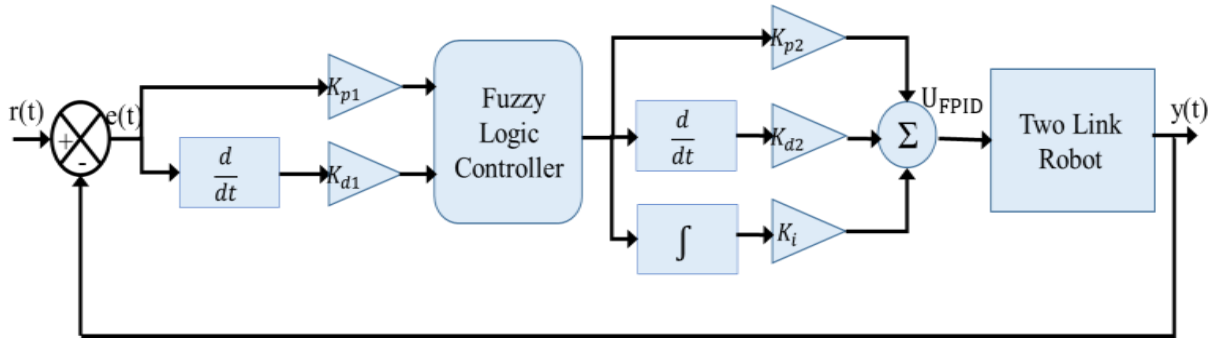

Figure. 6 The structure of the Fractional/Integer order fuzzy PD- Fractional/Integer order PID controller for 2-LRRM

3.2.1. Fractional/Integer order fuzzy PD + I controller design (FOFPD+I/IOFPD+I)

The Fractional/Integer Order fuzzy PD+I controller general block structure of 2-LRRM for trajectory tracking is shown in Fig.3.

This figure represents the individual controller for each input of 2-LRRM controlling, where the reference trajectory is compared with the actual trajectory for each link. The error e and its change ė are the input variables for the basic fuzzy controller.

The fuzzy controller has only a fuzzy proportional-differential control block. It does not have a fuzzy integral control block. The Integral Control (IC) is merged with the fuzzy PD controller to improve the steady-state performance of the system [20].

3.2.2. One block fractional/Integer order fuzzy PID controller design (OBFOFPID/OBIOFPID)

The separate controller for each input of 2-LRRM controlling of the One Block Fractional/Integer Order Fuzzy PID controller is shown in Fig. 4.

This controller is formed as a summation of the fuzzy PD controller output and the fuzzy PI controller output while the output of the fuzzy PD will be fed to the integrator to form a fuzzy PI controller. The standard fuzzy PID controller is constructed by choosing the inputs to be error e and derivative of the error ė and the output to be the control signal u [21]

3.2.3. Two block Fractional/Integer order fuzzy PID controller design (TBFOFPID/TBIOFPID)

The Two-Block Fractional/Integer Order Fuzzy PID controller general structure is shown in Fig. 5. This figure represents the individual controller for each input of 2-LRRM controlling.

Since it is difficult for the fuzzy PD to remove the steady-state error, it is known that the feasibility of the fuzzy PI control is more than that of the fuzzy PD control. The fuzzy PI control type is well-known for its poor transient response performance due to the inner integration process. A fuzzy PID is used to retain the precise features of the PID controller while merging the performance of fuzzy PI control and fuzzy PD control at the same time [22].

Table 2. Rule base for an error, derivative error, and FLC output

ė \ e	**NL**	**NM**	**NS**	**Z**	**PS**	**PM**	**PL**
NL	NL	NL	NL	NL	NM	NS	Z
NM	NL	NL	NL	NM	NS	Z	PS
NS	NL	NL	NM	NS	Z	PS	PM
Z	NL	NM	NS	Z	PS	PM	PL
PS	NM	NS	Z	PS	PM	PL	PL
PM	NS	Z	PS	PM	PL	PL	PL
PL	Z	PS	PM	PL	PL	PL	PL

3.2.4. Fractional/Integer order fuzzy PD-Fractional/Integer order PID controller design (FOFPD-FOPID/IOFPD-IOPID)

The separate controllers for each input of the 2-LRRM controlling of the Fractional/Integer Order Fuzzy PD- Fractional/Integer Order PID controller are shown in Fig. 6. The fuzzy controller uses error e and derivative of error ė as input signals. This controller is constructed from fuzzy PD and PID controller in which the output of the fuzzy PD will be input to the PID controller [23]

In this study seven Gaussian membership functions (MF), as "Negative large (NL)", "Negative Medium (NM)", "Negative Small (NS)", "Zero (Z)", "Positive Small (PS)", "Positive Medium (PM)" and at last "Positive Large (PL)" are used for each input signal e,ė and control signal U and the universe of discourse chosen to be [-10,10] where the rules in the rule base as shown in Table 2.

4. Most valuable player algorithm

The Most Valuable Player Algorithm (MVPA) is a recently generated algorithm suggested by Bouchekara 2017. It is motivated by sport, in which the group of players is organized into teams, then the teams start competing to win the championship, inside each team, individual players are trying to win the most valuable player trophy by competing against each other [24].

MVPA has the following characteristics: it converges speedily, it is reliable, and it is efficient, To develop optimality, MVPA exploits a population, which is a group of skilled players that are similar to the design variables in which the number of the player's skills corresponds to the problem dimension, a player is represented as following [25]:

$$\text{Player}_k = \left[S_{k,1} \quad S_{k,2} \ldots\ldots S_{k,\text{Problem Size}}\right] \quad (18)$$

The collection of players constricts a group or a team which is given by:

$$\text{TEAM}_i = \begin{bmatrix} \text{Player}_1 \\ \text{Player}_2 \\ \vdots \\ \text{Player}_{\text{Players Size}} \end{bmatrix} \quad (19)$$

Where S denotes the skill, Players Size is the number of players in the competition, and Problem Size is the problem dimension. Each team has its prim player (i.e., their current most skillful player). The competition's MVP is the finest player in the league (the player that has the best solution so far).

4.1 The most valuable player algorithm

1- Initialization: a population of Players Size, players are arbitrarily created in the search space.
2- Teams formation: once the players' population has been created, they are distributed randomly to form teams of Teams Size.
3- Competition phase: in this phase, each player is trying to enhance his skills separately to be the best player and then compete as teams, they play against one another. There are two steps: individual competition and team competition.
   - Individual competition: it is genuine that any player wants to be the best player for the team and the competition MVP. So, the player attempts to develop his abilities. Therefore, the players' skills of TEAM_i are reassessed as follows:

$$\begin{aligned}\text{skill}_i = \text{skill}_i &+ \text{rand} \\ &\times (\text{skill}(\text{Franchise Player}_i) \\ &- \text{skill}_i) + 2 \times \text{rand} \\ &\times (\text{skill}(\text{MVP}) - \text{skill}_i)\end{aligned} \quad (20)$$

Where a rand is a random number distributed randomly in the range [0 1], Franchise Player is the best player in the team.

   - Team competition: in this stage, another team TEAM_j is randomly selected, where $(i \neq j)$ then TEAM_i and TEAM_j compete against each other to decide the best team.

The Franchise Player fitness represents the team fitness and it is normalized in the MVPA, by assessment as follows:

$$\begin{aligned}\text{fitnessN}(\text{TEAM}_i) = \text{fitness}(\text{TEAM}_i) \\ - \min\big(\text{fitness}(\text{All Teams})\big)\end{aligned} \quad (21)$$

Then, to calculate the probability that TEAM_i beats TEAM_j, the following formula is used:

$$\Pr\{\text{TEAM}_i \text{ beats TEAM}_j\} = 1 - \frac{(\text{fitnessN}(\text{TEAM}_i))^k}{(\text{fitnessN}(\text{TEAM}_i))^k + (\text{fitnessN}(\text{TEAM}_j))^k} \quad (22)$$

Finally, in the team competition phase if TEAM_i is chosen to play against TEAM_j, and TEAM_i wins, then TEAM_i player skills are reassessed by:

$$\text{skill}_i = \text{skill}_i + \text{rand} \times \left(\text{skill}_i - \text{skill}(\text{Franchise Player}_j)\right) \quad (23)$$

Otherwise, the TEAM_i players' skills are calculated by:

$$\text{Skill}_i = \text{skill}_i + \text{rand} \times \left(\text{skill}(\text{Franchise Player}_j) - \text{skill}_i\right) \quad (24)$$

It should be noted that the skills of the player have upper and lower limits, and all of the players are actively trying to enhance their skills in each competition. At any updating phase, if the player's skills go beyond their bound then it must be limited to the bound of skills. The checking of the player skills bound is performed regularly in a special stage that is called the bound checking stage.

4- Application of greediness: an assessment is done after each step of competition (individual and team competition). The population before and after the competition phase is compared in this assessment. If the results are better than that of the initial stage, the solution is accepted.
5- Application of elitism: the poorest players are substituted with the better ones in this phase. The number of elite players is chosen as the third of the Players Size.
6- Remove duplicates: in the population, if two consecutive players are the same, the subsequent player will be substituted by another player.
7- Termination criterion: the algorithm repeats several times. The number of iterations is specified by MaxNFix (maximum number of fixtures) [24, 25].

5. Simulation and result

The performance of trajectory tracking and the robustness of the FOFPID and IOFPID controllers are discussed in this section. The proposed controllers, the 2-LRRM, and test trajectory are simulated using MATLAB code. The simulation time is taken as 4s, while the sampling time is taken as 1ms. The orders of the proposed FOFPID controller can be adjusted to meet the design specifications and give flexibility in choosing the control constraints. Additionally, Grunewald's approximation of the 5th order (N=5) is used for the fraction operator design. Frequency range [0.001, 1000] rad/s is used with the approximation for the fractional operator design.

The trajectory tracking of each link is calculated so that the manipulator can follow it. The results then are used as a function of the performance index for each controller. The Integral of Time Square Error (ITSE) performance index is used in the test.

The MVPA was employed to regulate the constraints of FOFPID and IOFPID controllers according to the tracking error between the 2-LRRM real path and the reference path using two initial positions (0.1745, 0.1745) and (-0.1745,-0.1745) for θ_1 and θ_2 respectively. The MVPA setting is as follows; the population size=40, team size=5, team players =8, and the maximum number of iterations=300. The best solution resulting in the last iteration is taken as the result of MVPA. The performance assessment of FOFPID and IOFPID controllers is based on the computation of the ITSE, the best controller is the one that has the less value. The ITSE can be calculated using the following formula:

$$\text{ITSE} = \int \left(t \times e_1^2(t) + t \times e_2^2(t)\right) dt \quad (25)$$

Where $e_1(t)$ and $e_2(t)$ are the difference between the desired and real trajectories for link_1 and link_2 respectively. The desired trajectories θ_{r1} and θ_{r2} for link_1 and link_2 have been given in Eqs. (26) and (27), respectively as follows:

$$\theta_{r1} = \begin{cases} 0.75 \times t^2 - 0.25 \times t^3 & ,0 < t < 2 \\ -1.5 + 3 \times t - 1.125 \times t^2 + 0.125 \times t^3 & ,2 < t < 4 \end{cases} \quad (26)$$

$$\theta_{r2} = \begin{cases} 1.5 \times t^2 - 0.5 \times t^3 & ,0 < t < 2 \\ 12 - 12 \times t + 4.5 \times t^2 - 0.5 \times t^3 & ,2 < t < 4 \end{cases} \quad (27)$$

The best values for all proposed controllers gains resulting from the last iteration of MVPA are shown in Table 3, and the corresponding ITSE of these controllers as in Table 4. In general, the ITSE values for the FOFPID controllers are lower than that of IOFPID controllers in all structures and the FOFPD-FOPID gives the less value of ITSE among all FOFPID controllers. The drawing of trajectory

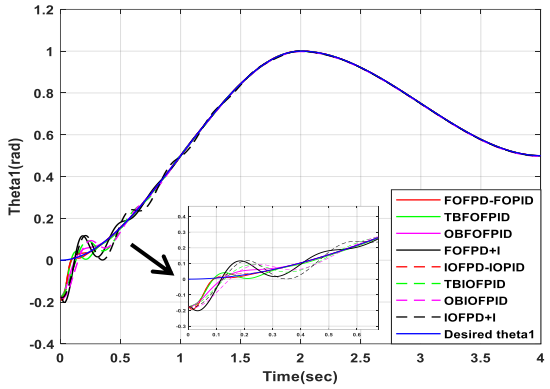

(a)

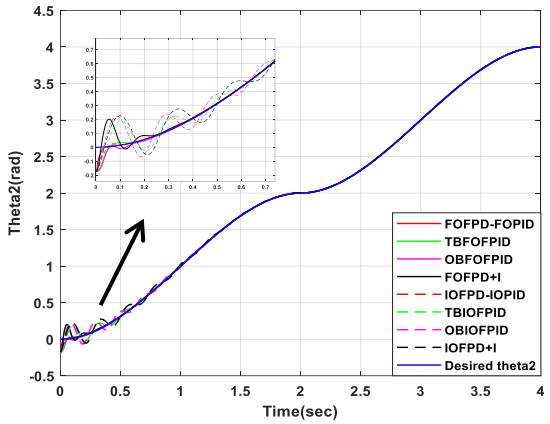

(b)

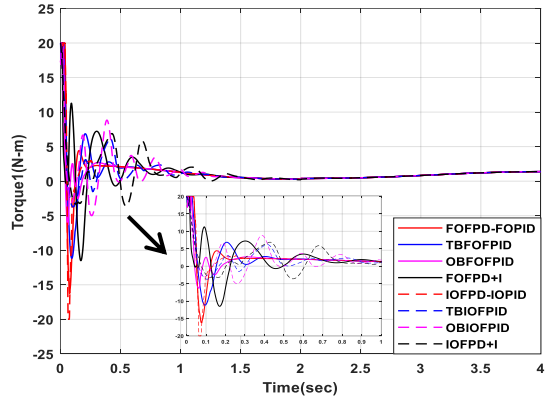

(c)

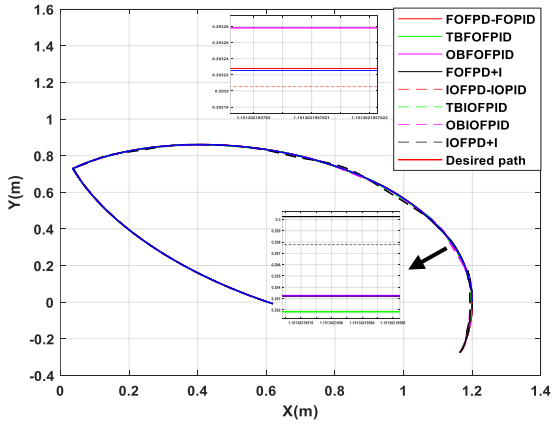

(d)

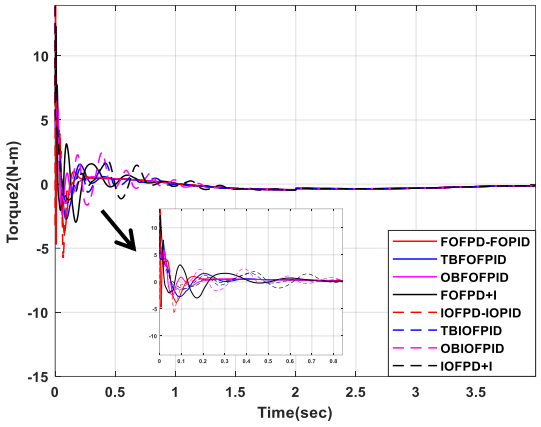

(e)

Figure. 7 (a) Desired and actual theta1, (b) Desired and actual theta2, (c) Desired and actual paths, (d) Controller output (torqu1), and (e) Controller output (torqu2)

tracking of theta1 and theat2, the path traced by the end-effector of the 2-LRRM, and controller output are presented in Fig. 7.

It is clear from previous results that the response of the trajectory tracking for theta1 and theta2 without overshoot and it has minimum settling time in case of FOFPD-FOPID controller, while it has maximum overshoot and maximum settling time in case of IOFPD+I.

To check the robustness of the FOFPID and IOFPID controllers, another primary position such as [0.15, 0.15] for $[\theta_1,\theta_2]$, is taken to test the ability of the suggested controllers to track the two-link robot on the chosen path. The obtained result is shown in Table 5. Fig. 8 shows the trajectory tracking of theta1 and theta2 and the path tracked by the end-effector of the 2-LRRM with changing the initial position for all controllers.

Despite changing the initial positions, the FOFPD-FOPID controller remains the best performer than the rest, since there is no overshoot in the response of trajectory tracking of theta1 and theta2 and the settling time is the minimum. While the IOFPD+I is the worst because the response of theta1 and theta2 has maximum overshoot and maximum settling time.

Another test for the robustness of the FOFPID and IOFPID controllers by adding disturbance term [sin (50t), sin (50t)] to the control action $[\tau_1,\tau_2]$, and making the initial position as [0, 0], without retraining the parameters (gains) of FOFPID and IOFPID controllers to confirm the robustness and the ability of each controller.

The obtained result is shown in Table 6. The trajectory tracking of theta1 and theta2 and the path

Table 3. The gains of the FOFPID and IOFPID controllers

Controller	Link NO	K_p	K_d	K_i	K_o	μ	λ
FOFPD-FOPID	L1	K_{p1}= -10.1724 K_{p2}= 9.9166	K_{d1}= -11.4738 K_{d2}= 5.8532	37.9654	-	μ_1 = 0.0329 μ_2 = 0.7617	0.0888
	L2	K_{p1}= -15.0553 K_{p2}= 47.7082	K_{d1}= -12.4056 K_{d2}= 9.7917	34.2747	-	μ_1 = 0.0488 μ_2 = 0.9997	0.0179
IOFPD-IOPID	L1	K_{p1}= 28.2710 K_{p2}= -23.0416	K_{d1}= -25.5490 K_{d2}= -1.1712	0.2352	-	-	-
	L2	K_{p1}= -20.8094 K_{p2}= 28.0464	K_{d1}= 26.5808 K_{d2}= 1.8930	-0.0294	-	-	-
TBFOFPID	L1	K_{p1}= -6.4796 K_{p2}= -10.1531	K_{d1}= -2.8004 K_{d2}= -15.5898	18.6482	11.0377	0.4778	0.0933
	L2	K_{p1}= 10.7877 K_{p2}= -4.2935	K_{d1}= 0.1559 K_{d2}= -6.3977	-12.7727	19.4736	0.7859	0.2110
TBIOFPID	L1	K_{p1}= - 4.0141 K_{p2}= -2.3489	K_{d1}= -52.2225 K_{d2}= -96.6613	- 2.6777	94.8572	-	-
	L2	K_{p1}= 8.2145 K_{p2}= 8.1349	K_{d1}= 95.1769 K_{d2}= 97.9022	31.6260	-90.1372	-	-
OBFOFPID	L1	15.3138	3653.4	6.7374	-15.2112	0.8333	0.0634
	L2	15.5876	30.1463	12.2027	-30.3515	0.4419	0.4772
OBIOFPID	L1	-1.1310	-51.7489	-31.1856	195.3759	-	-
	L2	5.9723	55.5988	16.1857	-134.7754	-	-
FOFPD+I	L1	9.7843	6.9423	45.2943	-17.7013	0.3997	0.0615
	L2	15.4913	5.5418	106.0475	-53.5378	0.5381	0.0240
IOFPD+I	L1	-2.5888	-57.3065	17.0627	100.7910	-	-
	L2	5.6015	57.3065	36.7680	-109.9999		-

Table 4. The ITSE of the FOFPID and IOFPID controllers

controller	ITSE	controller	ITSE
FOFPD-FOPID	7.7481 $\times 10^{-5}$	IOFPD-IOPID	1.0129 $\times 10^{-4}$
TBFOFPID	1.5261 $\times 10^{-4}$	TBIOFPID	1.6378 $\times 10^{-3}$
OBFOFPID	2.5903 $\times 10^{-4}$	OBIOFPID	2.4 2013$\times 10^{-3}$
FOFPD+I	6.9568 $\times 10^{-4}$	IOFPD+I	4.4573 $\times 10^{-3}$

Table 5. The ITSE of the FOFPID and IOFPID with initial position (0.15, 0.15)

controller	ITSE	controller	ITSE
FOFPD-FOPID	2.4334 $\times 10^{-5}$	IOFPD-IOPID	4.2157 $\times 10^{-5}$
TBFOFPID	5.1637 $\times 10^{-5}$	TBIOFPID	6.1976 $\times 10^{-4}$
OBFOFPID	1.1887 $\times 10^{-4}$	OBIOFPID	8.5812 $\times 10^{-4}$
FOFPD+I	1.8352 $\times 10^{-4}$	IOFPD+I	1.8 $\times 10^{-3}$

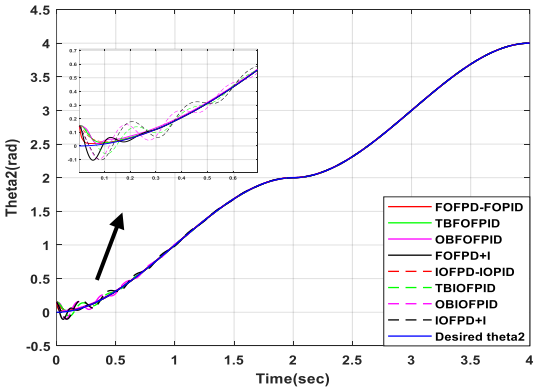

(a)

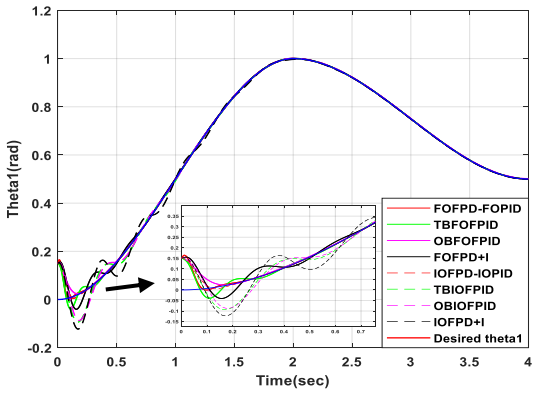

(b)

tracked by the end-effector of the 2-LRRM using disturbance of sin50t N-m in both links are presented in Fig. 9.

From the results, we conclude that the FOFPID controller functions better for the disturbances rejection also when comparing it to the other IOFPID controllers, where the FOFPD-FOPID is the best one since it has the smallest ITSE.

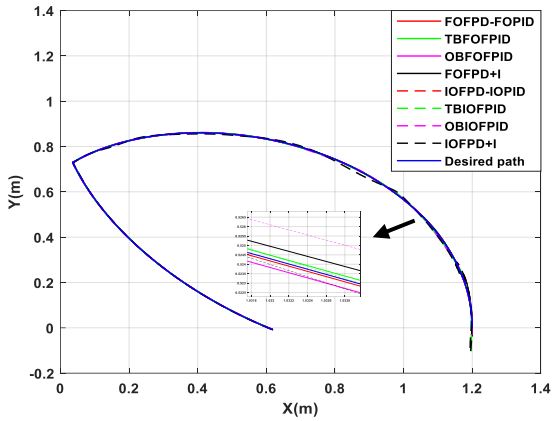

(c)

Figure. 8 (a) Desired and actual thata1, (b) Desired and actual theta2, and (c) Desired and actual paths with initial positions (0.15,0.15)

Table 6. The ITSE of the FOFPID and IOFPID with disturbances sin (50t) for both links and Initial position(0,0)

controller	ITSE	controller	ITSE
FOFPD-FOPID	2.1893 $\times 10^{-4}$	IOFPD-IOPID	1.2 $\times 10^{-3}$
TBFOFPID	2.3 $\times 10^{-3}$	TBIOFPID	5.1 $\times 10^{-3}$
OBFOFPID	1.3 $\times 10^{-3}$	OBIOFPID	6 $\times 10^{-3}$
FOFPD+I	4.5 $\times 10^{-3}$	IOFPD+I	6.4 $\times 10^{-3}$

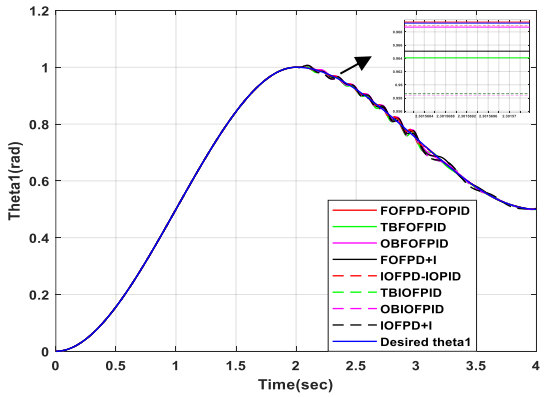

(a)

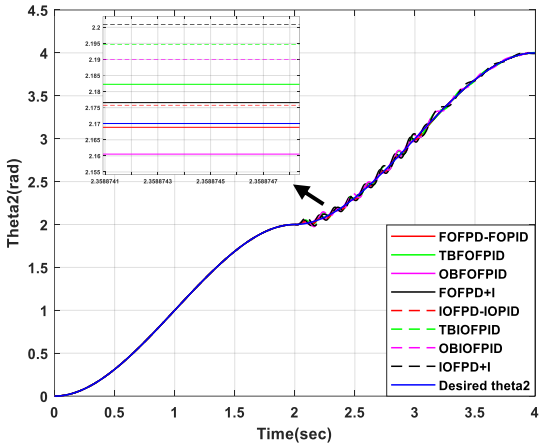

(b)

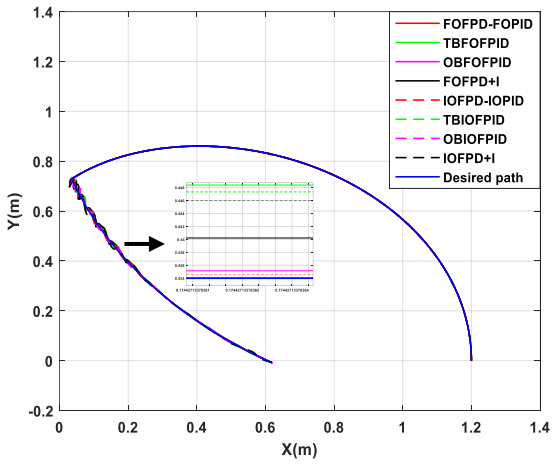

(c)

Figure. 9 (a) Desired and actual theta1, (b) Desired and actual theta2, and (c) Desired and actual paths with disturbance term [sin (50t), sin (50t)] and initial position (0, 0)

Table 7. The ITSE of the FOFPID and IOFPID for 5% increase in both masses and initial position (0,0)

controller	ITSE	controller	ITSE
FOFPD-FOPID	2.4990 $\times 10^{-6}$	IOFPD-IOPID	8.4663 $\times 10^{-6}$
TBFOFPID	7.3864 $\times 10^{-5}$	TBIOFPID	1.2744 $\times 10^{-4}$
OBFOFPID	8.6453 $\times 10^{-5}$	OBIOFPID	1.0589 $\times 10^{-4}$
FOFPD+I	3.5313 $\times 10^{-5}$	IOFPD+I	5.9906 $\times 10^{-5}$

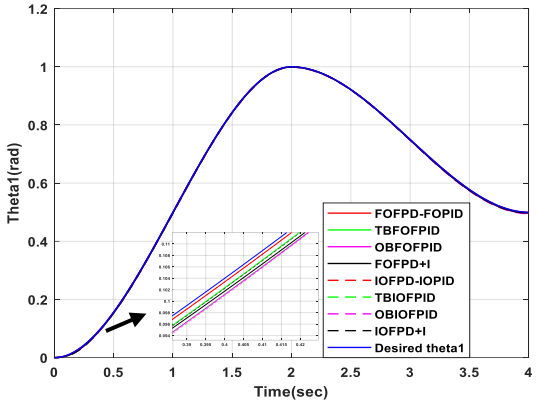

(a)

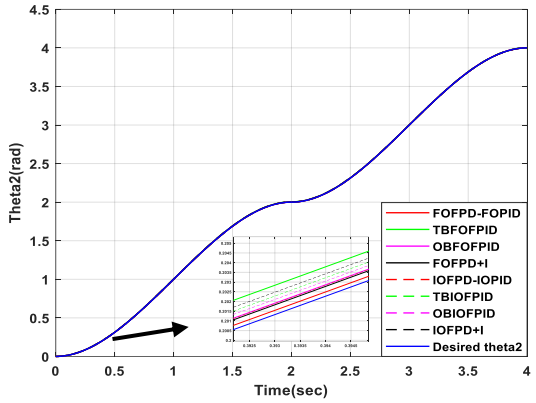

(b)

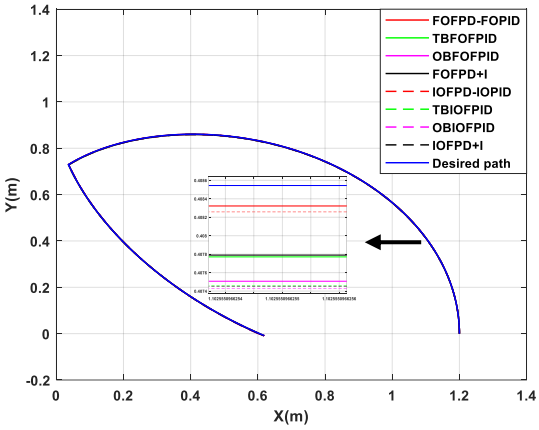

(c)

Figure. 10 (a) Desired and actual theta1, (b) Desired and actual theta2, and (c) Desired and actual paths for 5% increase in both masses and initial position (0, 0).

The parameter variation is also investigated for the FOFPID and IOFPID controllers, by increasing the masses of two links 5%, the results as in Table 7, and the trajectory tracking of theta1 and theta2 and the path tracked by the end-effector of the 2-LRRM for mass changes for all controllers are presented in Fig. 10.

From the results presented, it can be deduced that in general FOFPID controllers outperforms the IOFPID controllers for parameter variation and the best controller is FOFPD-FOPID among them.

The effect of adding disturbance and parameter variation as well as changing the initial positions together on the FOFPID and IOFPID controllers is presented in Table.8. Fig.11 shows the trajectory tracking of theta1 and theta2 and the path tracked by the end-effector of the 2-LRRM for disturbance, parameter variation as well as changing the initial positions for all controllers.

Table 8. The ITSE of the FOFPID and IOFPID with initial position (0.15, 0.15), disturbances sin (50t) for both links, and a 5% increase in both masses

controller	**ITSE**	**controller**	**ITSE**
FOFPD-FOPID	2.4470 $\times 10^{-4}$	IOFPD-IOPID	1.1 $\times 10^{-3}$
TBFOFPID	2.2 $\times 10^{-3}$	TBIOFPID	5.6 $\times 10^{-3}$
OBFOFPID	1.7 $\times 10^{-3}$	OBIOFPID	6.4 $\times 10^{-3}$
FOFPD+I	4.5 $\times 10^{-3}$	IOFPD+I	7.8 $\times 10^{-3}$

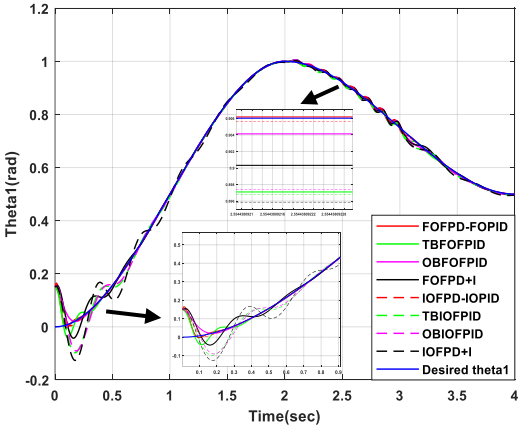

(a)

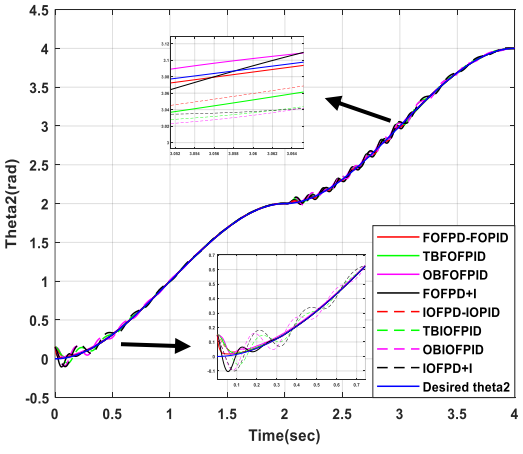

(b)

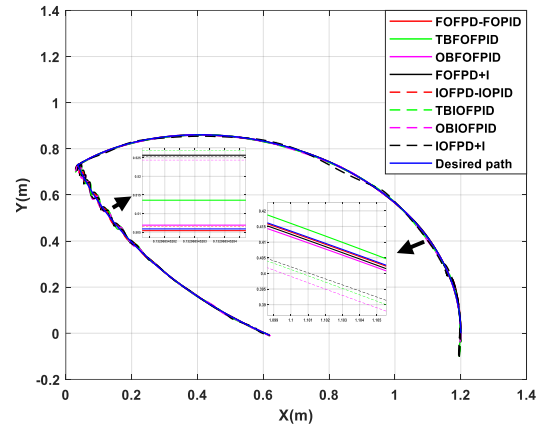

(c)

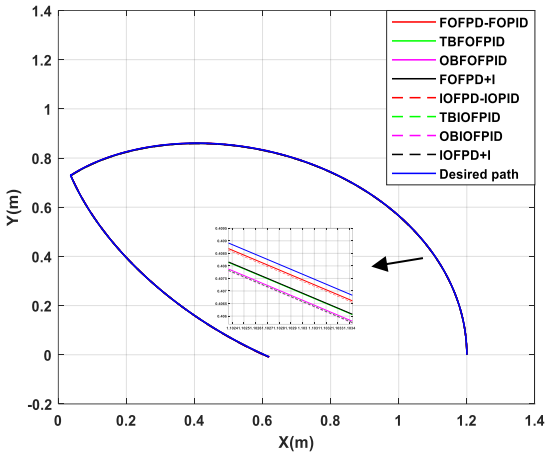

Figure. 11 (a) Desired and actual theta1, (b) Desired and actual theta2, (c) Desired and actual paths with initial position (0.15, 0.15), disturbance term [sin (50t), sin (50t)] and 5% increasing in both masses

Table 9. Comparison between proposed FOFPID controllers and existing controllers for trajectory tracking

Type of controller	IAE1	IAE2
FOFPD-FOPID	1.0187×10^{-5}	2.0433×10^{-5}
TBFOFPID	2.8295×10^{-5}	1.6388×10^{-4}
OBFOFPID	5.1976×10^{-5}	7.1157×10^{-5}
FOFPD+I	3.9962×10^{-5}	5.0123×10^{-5}
FOFPID [5]	4.632×10^{-4}	4.180×10^{-5}
2 DOF FOFPI-D [7]	9.086×10^{-4}	5.748×10^{-4}

It is found that the ITSE for FOFPD-FOPID controller remains the smallest among proposed controllers despite changing initial conditions, adding disturbance, and parameter variation, and we can show from the response of theta1 and theta2 there is no overshoot and it has a minimum settling time while the worst controller is the IOFPD+I.

Another comparison is done among FOFPID controllers proposed in this work and the FOFPID, 2DOF FOFPI-D controllers that were used to control the 2- link robot manipulator in [5] and [7]. The comparison was done in the case of trajectory tracking by using Integral Absolute Error (IAE) for link1 and lonk2 which are given in Eqs. (28) and (29), respectively, and the results listed in Table 9. The results show that the IAE for the proposed FOFPID controllers are better or converge with the best data obtained from the existing controllers.

$$\text{IAE1} = \int |e_1(t)|\,\text{dt} \tag{28}$$

$$\text{IAE2} = \int |e_2(t)|\,\text{dt} \tag{29}$$

6. Conclusion

In this paper, four structures of FOFPID and IOFPID controllers were proposed for a 2-LRRM for trajectory tracking problems. The addition of the fractional operator to the FPID controller has given control engineers more design flexibility because it adds two more variables to tune. A metaheuristic MVPA is used to tune controllers' parameters. Furthermore, the robustness of these controllers has been explored for initial conditions, disturbance rejection, and model uncertainty. The results show that the FOFPID controllers have a respectable capability to reduce the variance between real and desired paths speedily and then to track the wanted path with good accurateness and without chattering in control signals, where the best controller is the FOFPD-FOPID, the next is the TBFOFPID, after that the OBFOFPID and at last the FOFPD+I.

It can be concluded that the FOFPID controllers are better and more robust than the IOFPID controllers in all structures, whereas the ITSE for FOFPD-FOPID, TBFOFPID, OBFOFPID, and FOFPD+I for trajectory tracking task equal to 7.7481×10^{-5}, 1.5261×10^{-4}, 2.5903×10^{-4}, and 6.9568×10^{-4} respectively, while the ITSE for IOFPD-IOPID, TBIOFPID, OBIOFPID, IOFPD+I equal to 1.0129×10^{-4}, 1.6378×10^{-3}, 2.42013×10^{-3} and 4.4573×10^{-3} respectively. FOFPD-FOPID controller is the best among all studied controllers for trajectory tracking , disturbance rejection , and parameter variation with superior trajectory tracking and the smallest ITSE. Also the result showed that the response of the trajectory tracking for theta1 and theta2 without overshoot and it has minimum settling time. This work also demonstrates the capability of MVPA for tuning the parameters of 2-LRRM controllers.

Finally, as future work, other optimization techniques can be used instead of MVPA such as ant colony optimization (ACO), genetic algorithm (GA), and differential search algorithm (DSA) to tune the parameters of the controllers. Besides, Implementing the suggested controllers practically by using a real robot manipulator with all necessary hardware.

Conflicts of Interest

The authors declare that they have no known competing financial interests or personal relationships that could have appeared to influence the work reported in this paper

Author Contributions

Conceptualization,1st author; methodology,1st author; software, 2nd author; validation, 1st author; formal analysis, 1st author; investigation, 1st author; resources, 1st author; data curation, 1st author; writing—original draft preparation, 1st author; writing—review and editing, 1st author; visualization, 1st author; supervision, 2nd author; project administration, 2nd author.

Acknowledgments

This work was supported by the Department of Control and Systems Engineering /University of technology-Iraq.

References

[1] A. M. Mustafa and A. A. Saif, "Modeling, Simulation, and Control of 2-R Robot", *Global Journal of Researches in Engineering: H Robotics and Nano-Tech*, Vol. 14, pp. 3360-3366, 2014.

[2] Y. J. Huang, "Variable structure control for a two-link robot arm", *Electrical Engineering*, Vol. 85, No. 4, pp. 195-204, 2003.

[3] Z. Dachang, D. Baolin, Z. Puchen, and C. Shouyan, "Constant Force PID Control for Robotic Manipulator Based on Fuzzy Neural Network Algorithm", *Complexity*, Vol. 2020, 2020.

[4] M. Manjeet and S. Sathans, "Fuzzy based Control of Two Link Robotic Manipulator and Comparative Analysis", *International Conference on Communication Systems and Network Technologies Fuzzy*, pp. 562-567, 2013.

[5] R. Sharma, K. P. S. Rana, and V. Kumar, "Performance analysis of fractional-order fuzzy PID controllers applied to a robotic manipulator", *Expert Systems with Applications*, Vol. 41, No. 9, pp. 4274-4289, 2014.

[6] B. Rahmani and M. Belkheiri, "Robust Adaptive Control of Robotic Manipulators Using Neural Networks: Application to a Two Link Planar Robot", In: *Proc. of International Conf. on Modelling, Identification, and Control*, pp. 839-844, 2016.

[7] V. Mohan, H. Chhabra, A. Rani, and V. Singh, "An expert 2DOF fractional order fuzzy PID controller for nonlinear systems", *Neural Computing and Applications*, Vol. 31, No. 8, pp. 4253-4270, 2018.

[8] A. O. P. Lerma, R. G. Hernandez, V. Santibanez, and J. V. Chin, "Experimental Evaluation of a Sectorial Fuzzy Controller Plus Adaptive Neural Network Compensation Applied to a 2-DOF Robot Manipulator", *International Federation of Automatic Control PapersOnLine*, Vol. 52, No. 29, pp. 233-238, 2019.

[9] H. A. R. Akkar and S. Q. G. Haddad, "Design Stable Controller for PUMA 560 Robot with PID and Sliding Mode Controller Based on PSO Algorithm", *International Journal of Intelligent Engineering and Systems*, Vol. 13, No. 6, pp. 487-499, 2020, doi: 10.22266/ijies2020.1231.43.

[10] H. Rahali, S. Zeghlache, and L. Benyettou, "Fault-Tolerant Control of Robot Manipulators Based on Adaptive Fuzzy Type-2 Backstepping in Attendance of Payload Variation", *International Journal of Intelligent Engineering and Systems*, Vol. 14, No. 4, pp. 312-325, 2021, doi: 10.22266/ijies2021.0831.28.

[11] B. Bandyopadhyay and S. Kamal, *Stabilization and Control of Fractional Order Systems: A Sliding Mode Approach*, Vol. 317, 2015.

[12] S. M. Raafat and F. A. Raheem, "Introduction to Robotics-Mathematical Issues", *Mathematical Advances Towards Sustainable Environmental Systems*, pp. 261-289, 2017.

[13] F. L. Lewis, D. M. Dawson, and C. T. Abdallah, *Robot Manipulator Control Theory and Practice*, *CRC Press*, pp. 1-632, 2004.

[14] K. H. Ang, G. Chong, and Y. Li, "PID Control System Analysis, Design, and Technology", *Transactions on Control Systems Technology*, Vol. 13, No. 4 .pp. 559-576, 2005.

[15] F. A. Raheem, B. F. Midhat, and H. S. Mohammed, "PID and Fuzzy Logic Controller Design for Balancing Robot Stabilization", *Iraqi Journal of Computers, Communications, Control and Systems Engineering*, Vol. 18, No.

1, pp. 1-10, 2018.
[16] H. Delavari, R. Ghaderi, N. Ranjbar, S. H. Hosseinnia, and S. Momani, "Adaptive Fractional PID Controller for Robot Manipulator", In: *Proc. of the 4th IFAC Workshop Fractional Differentiation and its Application*, Vol. 2010, pp. 1-7, 2010.
[17] H. M. Kadhim and A. A. Oglah, "Interval type-2 and type-1 Fuzzy Logic Controllers for congestion avoidance in internet routers", In: *Proc. of International Conf. on Sustainable Engineering Techniques*, Vol. 881, No. 1, p. 012135, 2020.
[18] D. M. Wonohadidjojo, G. Kothapalli, and M. Y. Hassan, "Position Control of Electro-hydraulic Actuator System Using Fuzzy Logic Controller Optimized by Particle Swarm Optimization", *International Journal of Automation and Computing*, Vol. 10, No. 3, pp. 181-193, 2013.
[19] W. I. M. A. Tameemi and W. M. H. Hadi, "Modeling and Control of 5250 Lab-Volt 5 DoF Robot Manipulator", *Iraqi Journal of Computers, Communication, Control and Systems Engineering*, Vol. 15, No. 2, pp. 34-46, 2015.
[20] J. R. B. A. Monteiro, W. C. A. Pereira, M. P. Santana, T. E. P. Almeida, G. T. Paula, and I. Santini, "Anti-windup method for fuzzy PD+ I, PI and PID controllers applied in brushless DC motor speed control", *Brazilian Power Electronics Conference*, pp. 865-871, 2013.
[21] A. Vasičkaninová, M. Bakošová, J. Oravec, and M. Horváthová, "Efficient Fuzzy Control of a Biochemical Reactor", *Chemical Engineering Transactions*, Vol. 81. pp. 85-90, 2020.
[22] M. J. Mohamed and M. Y. Abbas, "Design Interval Type-2 Fuzzy Like (PID) Controller for Trajectory Tracking of Mobile Robot", *Iraqi Journal of Computers, Communications, Control and Systems Engineering*, Vol. 19, No. 3, pp. 1-15, 2019.
[23] P. C. Pradhan, R. K. Sahu, and S. Panda, "Firefly algorithm optimized fuzzy PID controller for AGC of multi-area multi-source power systems with UPFC and SMES", *Engineering Science and Technology, an International Journal*, Vol. 19, No. 1. pp. 338-354, 2015.
[24] H. Khattab, A. Sharieh, and B. A. Mahafzah, "Most Valuable Player Algorithm for Solving Minimum Vertex Cover Problem", *International Journal of Advanced Computer Science and Applications*, Vol. 10, No. 8, pp. 159-167, 2019.
[25] H. R. E. H. Bouchekara, "Most Valuable Player Algorithm: a novel optimization algorithm inspired from sport", *Springer Berlin Heidelberg*, Vol. 20, No. 1, 2017.